JOURNAL OF GUIDANCE, CONTROL, AND DYNAMICS
Vol. 24, No. 4, July–August 2001

Eigenstructure vs Constrained H^∞ Design for Hypersonic Winged Cone

Poonsuk Lohsoonthorn,* Edmond Jonckheere,† and Scott Dalzell*
University of Southern California, Los Angeles, Los Angeles, California 90089-2563

A variant of the eigenstructure assignment is developed to decouple phugoid and short periodic oscillations in longitudinal control of the winged cone, a benchmark hypersonic vehicle with airbreathing propulsion. The new method consists in minimizing the H^∞ norm of some closed-loop transfer matrix incorporating the undesirable couplings subject to the constraint that the closed-loop poles are consistent with such specifications as the military standard flying qualities of piloted aircraft. This constrained H^∞ method, with proper frequency-dependent weights, provides, in an indirect manner, the eigenstructure assignment consistent with the specifications on the responses. This new method and the traditional eigenstructure assignment are compared.

I. Introduction

THE purpose of this study is to highlight some specific decoupling issues in longitudinal control of the newer generation of airbreathing launch vehicles in hypersonic regime. The so-called winged cone, a reusable launch vehicle concept still being considered by NASA, is chosen as benchmark model. Critical in longitudinal control is the placement of the closed-loop poles at locations specified by, for example, the military standard flying qualities of piloted aircraft (MILSPEC), along with the achievement of a certain degree of decoupling between the phugoid and the short-period modes. More specifically, because airbreathing vehicles are vulnerable to change in angle of attack, it is imperative to achieve accurate angle-of-attack control and decouple it from the phugoid mode.

This decoupling is traditionally achieved via the Shapiro eigenstructure assignment. In this paper, we develop an alternate approach based on transcribing the amount of undesirable coupling in terms of the H^∞ norm of some specific closed-loop transfer matrix and using genetic algorithms to achieve the least possible H^∞ norm subject to closed-loop poles specifications. Comparison results between the traditional Shapiro eigenstructure assignment and the constrained H^∞ method reveal that, for the latter to be an improved method, the frequency weighting should be carefully chosen.

The paper is organized as follows. Section II develops the winged-cone model and the fundamental decoupling issues. Section III is devoted to the traditional Shapiro eigenstructure assignment decoupling design. The major contribution of the paper is Sec. IV, where the constrained H^∞ design and its generic algorithm solution are developed. The various design methods are compared in Sec. V.

II. Winged-Cone Configuration and Fundamental Decoupling Issues

The benchmark example considered here is the winged-cone configuration described in Refs. 1–3. In the present case study, the problem is to design a full state longitudinal controller gain matrix K (Fig. 1) based on two different approaches. The first approach is the classical eigenstructure assignment. The second approach is the H^∞ design subject to eigenvalue constraints.

The winged-cone accelerator air vehicle consists of an axissymmetric conical forebody, a cylindrical engine nacelle section with engine modules all around the body, and a cone frustrum engine nozzle section. The linearized longitudinal model represents a flight condition for trimmed accelerated flight at Mach 8 and 86,000 ft. The system is described by the linear time-invariant matrix differential equation

$$\dot{\boldsymbol{x}}_c = A_c \boldsymbol{x}_c + B_c \boldsymbol{u}_c \tag{1}$$

where $\boldsymbol{x}_c$ is the state vector and $\boldsymbol{u}_c$ is the control effort vector. The A_c and B_c coefficient matrices are given by

$$A_c = \begin{bmatrix} 3.65e{-3} & -9.67e{-1} & 0.00 & -5.56e{-1} & -1.43e{-3} \\ -3.92e{-5} & -8.16e{-2} & 1.00 & -8.44e{-5} & 9.25e{-6} \\ 2.01e{-3} & 3.03 & -9.52e{-2} & 1.55e{-5} & -1.08e{-5} \\ 2.73e{-6} & 7.77e{-6} & 1.00 & -7.77e{-6} & -1.02e{-9} \\ 2.08e{-2} & -1.37e{+2} & 0.00 & 1.37e{+2} & 0.00 \end{bmatrix} \tag{2}$$

$$B_c = \begin{bmatrix} 9.70e{-2} & 7.60 \\ 3.35e{-2} & -2.09e{-3} \\ 1.08 & 0.00 \\ 0.00 & 0.00 \\ 0.00 & 0.00 \end{bmatrix} = [\boldsymbol{b}_e \quad \boldsymbol{b}_\eta] \tag{3}$$

The state vector and the control effort vector are:

$$\boldsymbol{x}_c = \begin{bmatrix} V \\ \alpha \\ q \\ \theta \\ h \end{bmatrix} = \begin{bmatrix} \text{incremental velocity, ft/s} \\ \text{incremental angle of attack, deg} \\ \text{pitch rate, deg/s} \\ \text{incremental pitch attitude, deg} \\ \text{incremental altitude, ft} \end{bmatrix} \tag{4}$$

$$\boldsymbol{u}_c = \begin{bmatrix} \delta e \\ \delta \eta \end{bmatrix} = \begin{bmatrix} \text{symmetric elevon deflection, deg} \\ \text{fuel equivalent ratio} \end{bmatrix} \tag{5}$$

The elevon and the fuel equivalent ratio actuators are modeled as first-order lags by

$$\begin{bmatrix} \dot{\delta}_e \\ \dot{\delta}_\eta \end{bmatrix} = \begin{bmatrix} -30 & 0 \\ 0 & -100 \end{bmatrix} \begin{bmatrix} \delta_e \\ \delta_\eta \end{bmatrix} + \begin{bmatrix} 30 & 0 \\ 0 & 100 \end{bmatrix} \begin{bmatrix} r_e \\ r_\eta \end{bmatrix} \tag{6}$$

where r_e and r_η are the command signals to the symmetric elevon and the fuel equivalent ratio, respectively.

Consider the linear time-invariant winged-cone model with full state feedback control K and reference signal $\boldsymbol{r}$:

$$\dot{\boldsymbol{x}} = A\boldsymbol{x} + B\boldsymbol{u} \tag{7}$$

$$\boldsymbol{u} = \boldsymbol{r} - K\boldsymbol{x} \tag{8}$$

Received 25 March 2000; revision received 21 September 2000; accepted for publication 2 October 2000.

*Graduate Student, Department of Electrical Engineering-Systems.

†Professor, Department of Electrical Engineering-Systems.

Table 1 Desired closed-loop eigenvalues

Eigenvalue	Frequency, rad/s	Damping ratio	Desired eigenvalue	Comment
1	0.25000	0.7000	$-0.1750 + j0.1785$	Phugoid mode
2	0.2500	0.7000	$-0.1750 - j0.1785$	Phugoid mode
3	10.0000	0.7000	$-7.0000 + j7.1414$	Short-period mode
4	10.0000	0.7000	$-7.0000 - j7.1414$	Short-period mode
5	0.1000	1.0000	-0.1000	Altitude mode
6	31.0000	1.0000	-31.0000	Elevon actuator mode
7	101.0000	1.0000	-101.0000	FER actuator mode

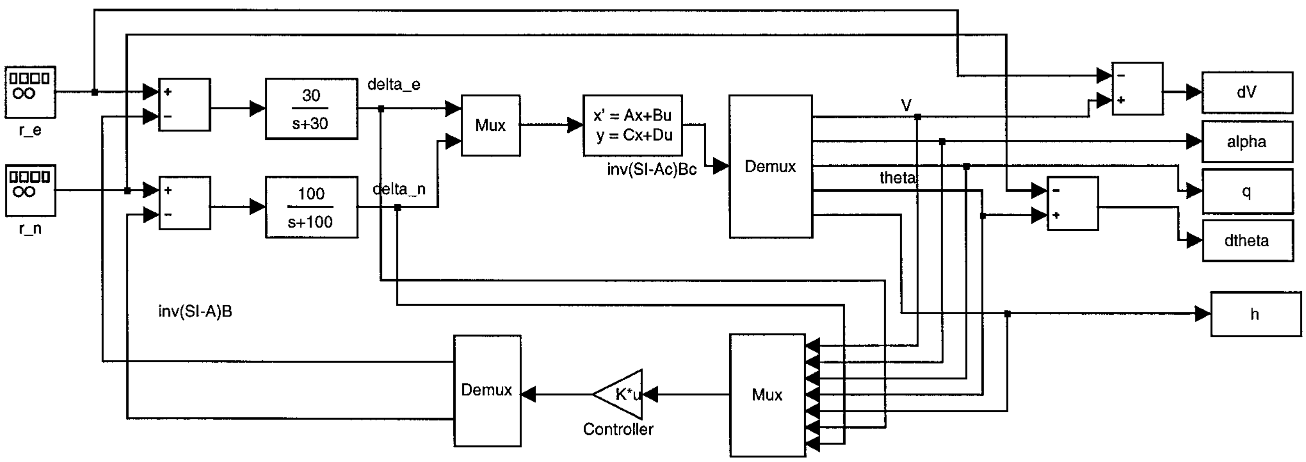

Fig. 1 Simulink block diagram of the overall controller design.

$$A = \begin{bmatrix} A_c & \boldsymbol{b}_e & \boldsymbol{b}_\eta \\ 0 & -30 & 0 \\ 0 & 0 & -100 \end{bmatrix} \tag{9}$$

$$B = \begin{bmatrix} 0 & 0 \\ 30 & 0 \\ 0 & 100 \end{bmatrix} = \begin{bmatrix} \boldsymbol{b}_{r_e} & \boldsymbol{b}_{r_\eta} \end{bmatrix} \tag{10}$$

$$\boldsymbol{x} = \begin{bmatrix} \boldsymbol{x}_c \\ \delta_e \\ \delta_\eta \end{bmatrix} \tag{11}$$

$$\boldsymbol{r} = \begin{bmatrix} r_e \\ r_\eta \end{bmatrix} \tag{12}$$

The eigenvalues of the A matrix are $\lambda_1^{ol} = -0.0009 + j0.0356$, phugoid mode; $\lambda_2^{ol} = -0.0009 - j0.0356$, phugoid mode; $\lambda_3^{ol} = -1.8312$, short-period mode; $\lambda_4^{ol} = 1.6533$, short-period mode; $\lambda_5^{ol} = 0.0065$, altitude mode; $\lambda_6^{ol} = -30.0000$, elevon actuator mode; and $\lambda_7^{ol} = -100.0000$, fuel equivalent ratio (FER) actuator mode, where the superscript ol stands for open loop.

Because the open-loop system is unstable due to the right half-plane eigenvalues λ_4 and λ_5, a controller is required to make the system stable and achieve acceptable responses. Performance objectives based on MILSPEC described in Refs. 4–6 are defined and used as a guideline for acceptable short-period and phugoid pole placement locations. The short-period mode specifications are

$$1.00 < \omega_n < 10.0, \qquad 0.35 < \xi < 1.30$$

and the phugoid mode specification is

$$0.10 < \xi$$

Based on these requirements, and because, for the altitude mode to remain decoupled, the altitude eigenvalue must be made neutrally or just slightly stable, the desired closed-loop characteristics were selected as in Table 1. (This choice of a stable altitude closed-loop pole λ_5 yields a controller for maneuvers and disturbance rejection at constant altitude. Relaxing the stability of λ_5 would yield a controller for such maneuvers as change of altitude, climbing, and so on. Because this is a different design philosophy and because, in general, the design is quite sensitive to the closed-loop poles, the case of a relaxed stability λ_5 is postponed to a later paper).

The desired eigenvectors are chosen such that, in the short-periodic eigenvectors $\boldsymbol{v}_3$ and $\boldsymbol{v}_4$, the angle of attack and the pitch rate are present while the velocity is decoupled. Moreover, the phugoid eigenvectors $\boldsymbol{v}_1$ and $\boldsymbol{v}_2$ are coupled with the pitch angle and the forward velocity while holding the angle of attack decoupled. This choice of eigenvectors is motivated by the flight dynamics of the problem, that is, during the short-period mode, the pitch angle is small and the velocity is constant, and during the phugoid mode, the angle of attack is constant. This yields a good degree of decoupling between these modes.

As we shall see, these eigenvector requirements produce the desirable feature that the throttle signal r_η controls the velocity V within the phugoid mode while all other short periodic state variables are unaffected. More important, the elevon signal r_e controls the angle of attack within the short-periodic mode while the phugoid state variables V and h are kept minimally affected. During this maneuver, though, the phugoid pitch angle variable θ is affected because of the constraint of holding the altitude decoupled, which yields $\gamma = \theta - \alpha = 0$ where γ is the flight-path angle.

In addition, the system must show acceptable response to initial angle-of-attack disturbance. Accurate angle-of-attack control, decoupled from the phugoid mode, is mandated by the requirement that the airflow to the airbreathing engine be kept uniform because otherwise the engine could stall.

To get a more accurate idea as to what the specifications in an airbreathing hypersonic vehicle are and how to go about matching them using the eigenstructure and H^∞ methods, observe that the closed-loop transfer matrix has a partial fraction decomposition of the form

$$(sI - A + BK)^{-1} = V_p W_p \frac{1}{s^2 - (\lambda_1 + \lambda_2)s + \lambda_1\lambda_2} + V_s W_s \frac{1}{s^2 - (\lambda_3 + \lambda_4)s + \lambda_3\lambda_4} + V_a W_a \frac{1}{s - \lambda_5} + V_e W_e \frac{1}{s - \lambda_6} + V_f W_f \frac{1}{s - \lambda_7}$$

In the preceding equation, the λ_i are the closed-loop eigenvalues, $[V_p\ V_s\ V_a\ V_e\ V_f]$ is the right eigenvectors matrix, the columns of which are the phugoid, short periodic, altitude, elevon, and FER modes, respectively, and

$$\begin{bmatrix} W_p \\ W_s \\ W_a \\ W_e \\ W_f \end{bmatrix}$$

is the matrix of row left eigenvectors taken in the same order. Moreover, the right and left eigenvectors are normalized as $W_k V_k = I$. The response to a unit step reference signal $r(s) = 1/s$, where r could be either r_e or r_η and $\boldsymbol{b}$ could be either $\boldsymbol{b}_{r_e}$ or $\boldsymbol{b}_{r_\eta}$, is given by

$$x(s) = (sI - A + BK)^{-1}\boldsymbol{b}r(s) = \left(V_p W_p \boldsymbol{b} \frac{1}{\lambda_1\lambda_2} + V_s W_s \boldsymbol{b} \frac{1}{\lambda_3\lambda_4} - V_a W_a \boldsymbol{b} \frac{1}{\lambda_5} - V_e W_e \boldsymbol{b} \frac{1}{\lambda_6} - V_f W_f \boldsymbol{b} \frac{1}{\lambda_7} \right) \frac{1}{s} + V_p W_p \boldsymbol{b} \frac{R_p s + S_p}{s^2 - (\lambda_1 + \lambda_2)s + \lambda_1\lambda_2} + V_s W_s \boldsymbol{b} \frac{R_s s + S_s}{s^2 - (\lambda_3 + \lambda_4)s + \lambda_3\lambda_4} - V_a W_a \boldsymbol{b} \frac{1}{\lambda_5(s - \lambda_5)} - V_e W_e \boldsymbol{b} \frac{1}{\lambda_6(s - \lambda_6)} - V_f W_f \boldsymbol{b} \frac{1}{\lambda_7(s - \lambda_7)}$$

where R_p, S_p, R_s, and S_s are residues.

Now, consider the problem of tracking an angle-of-attack reference signal, namely, $\boldsymbol{b}r = \boldsymbol{b}_{r_e} r_e$. To have an acceptable response where $\alpha(t)$ climbs to its steady-state value

$$\left[V_p W_p \boldsymbol{b}_e \left(1/\omega_p^2\right) + V_s W_s \boldsymbol{b}_e \left(1/\omega_s^2\right) - V_a W_a \boldsymbol{b}_e (1/\lambda_5) - V_e W_e \boldsymbol{b}_e (1/\lambda_6) - V_f W_f \boldsymbol{b}_e (1/\lambda_7) \right]_2$$

with the fast closed-loop short periodic dynamics, the crucial decoupling requirement is to keep the phugoid component of α small, that is,

$$\left(V_p W_p \boldsymbol{b}_{r_e} \right)_2 = (V_p)_2 W_p \boldsymbol{b}_{r_e}$$

In the traditional Shapiro eigenstructure assignment, this is accomplished by keeping the second component of V_p small, as shown in Table 2 (although no control is directly exercised over W_p). The traditional eigenstructure assignment is developed in Sec. III. On the other hand, to keep $(V_p W_p \boldsymbol{b}_{r_e})_2$ small using H^∞ methods, the guiding idea is to minimize the H^∞ norm of the transfer function:

$$W_p(s) C_\alpha (sI - A + BK)^{-1} \boldsymbol{b}_{r_e}, \qquad C_\alpha = [0 \quad 1 \quad 0 \quad 0 \quad 0 \quad 0 \quad 0]$$

where $W_p(s)$ is a bandpass filter around the phugoid mode to weight the undesirable component $C_\alpha V_p W_p \boldsymbol{b}_{r_e}$ more heavily than the desirable component $C_\alpha V_s W_s \boldsymbol{b}_{r_e}$.

Table 2 Desired eigenvectors

Parameter	V_p		V_s		V_a	V_e	V_f
Eigenvector	v_1	v_2	v_3	v_4	v_5	v_6	v_7
Velocity	x[a]	1[b]	0[c]	0	0	x	x
Angle of attack	0	0	x	1	x	x	x
Pitch rate	x	x	1	x	x	x	x
Pitch attitude	1	x	x	x	x	x	x
Altitude	x	x	x	x	1	x	x
Symmetric elevon	x	x	x	x	x	1	0
Fuel equivalent ratio	x	x	x	x	x	0	1

[a]Here x is an unspecified component.
[b]Here 1 means that some coupling should be present.
[c]Here 0 means that there should be no coupling.

A similar analysis can be done to achieve a free response to an angle-of-attack initial condition, decoupled from the phugoid mode. In this case, we minimize the H^∞ norm of

$$W_p(s) C_\alpha (sI - A + BK)^{-1} [0 \quad 1 \quad 0 \quad 0 \quad 0 \quad 0 \quad 0]^T$$

This is essentially the case study of Sec. V.

A dual analysis can also be done to secure a velocity response to $\boldsymbol{b}_{r_\eta}$ decoupled from the short periodic. Traditionally, this is achieved by keeping

$$(V_s W_s \boldsymbol{b}_\eta)_1 = (V_s)_1 \left[W_s \boldsymbol{b}_{r_\eta} \right]$$

small. The specification of a small V_s is shown by the two 0s appearing on the velocity components of the short-period eigenvectors v_3 and v_4. On the other hand, using H^∞ techniques, we minimize

$$W_s(s) C_V (sI - A + BK)^{-1} \boldsymbol{b}_\eta$$

where $W_s(s)$ is a bandpass filter around the short period.

III. Eigenstructure Assignment Using Full State Feedback

The first and most traditional method to decouple is to design the controller gain matrix by eigenstructure assignment using full state feedback. The eigenstructure design consists in placing the closed-loop eigenvalues according to such specifications as shown in Table 1 and the desired eigenvectors based on such structure as shown in Table 2.

The classical algorithm for the eigenstructure assignment can be described as follows. Consider a linear time-invariant system with full state feedback control as described by Eqs. (7–12), where $\boldsymbol{x} \in R^{n \times 1}$ is the state vector, $\boldsymbol{u} \in R^{m \times 1}$ is the control input vector, $A \in R^{n \times n}$, $B \in R^{n \times m}$, and $K \in R^{m \times n}$ is the state feedback gain matrix. In the eigenstructure assignment using full state feedback, we assume that the sets of open-loop eigenvalues and desired closed-loop eigenvalues are disjoint. Moreover, the desired eigenvalues are distinct. Hence, the closed-loop eigenvector equations are

$$(\lambda_i I - A + BK) v_i = 0, \qquad (\lambda_i I - A) v_i = -BK v_i \tag{13}$$

or, equivalently,

$$v_i = (\lambda_i I - A)^{-1} B \boldsymbol{u}_i \tag{14}$$

$$\boldsymbol{u}_i = -K v_i \tag{15}$$

where $i = 1, 2, \ldots, n$ and $\boldsymbol{u}_i \in R^{m \times 1}$. Because pairwise distinct eigenvalues will have linearly independent eigenvectors, the parametric representation of the control matrix K is given by

$$K = -U V^{-1} \tag{16}$$

where $U = [\boldsymbol{u}_1, \boldsymbol{u}_2, \ldots, \boldsymbol{u}_n]$ and $V = [v_1, v_2, \ldots, v_n]$. The eigenstructure method is to choose U such that the eigenvectors have some desired structure. In general, the desired eigenvectors do not reside in the subspace generated by the columns of the matrix $(\lambda_i I - A)^{-1} B$. Hence, we use a weighted least-squares fit method to obtain the best possible choice of the achievable eigenvectors. First, we consider the desired eigenvector $\boldsymbol{v}_i^d$ corresponding the eigenvalue λ_i. Then, we minimize the cost function

$$J = \sum_{i=1}^{n} \left(\boldsymbol{v}_i^d - L_i \boldsymbol{u}_i\right)^H R_i \left(\boldsymbol{v}_i^d - L_i \boldsymbol{u}_i\right) \tag{17}$$

relative to $\boldsymbol{u}_1, \boldsymbol{u}_2, \ldots, \boldsymbol{u}_n$, where

$$L_i = (\lambda_i I - A)^{-1} B \tag{18}$$

and R_i is a suitably adjusted symmetric positive semidefinite weighting matrix. It is adjusted to penalize the mismatch along the directions for which there is a hard specification (0,1) and not to penalize along the unspecified x directions. The solution of the weighted least-squares problem is

$$\boldsymbol{u}_i = \left(L_i^H R_i L_i\right)^{-1} L_i^H R_i \boldsymbol{v}_i^d \tag{19}$$

IV. Genetic Algorithms Parametric H^∞ Design Optimization

The new method consists in achieving a decoupling between the short-period mode and the phugoid mode based on parametric eigenvalues assignment where the freedom left beyond eigenvalues assignment is used to minimize the H^∞ norm of a transfer function matrix representing the couplings to be destroyed.

A. Parametric Eigenvalue Assignment

The parametric eigenvalue assignment is due to Liu and Patton.[7–9] This procedure for parametric eigenvalue assignment can be paraphrased, for the case of simple closed-loop eigenvalues in accordance with MILSPEC, as follows (see Liu and Patton[7–9]).

Define a closed-loop self-conjugate eigenvalue set $\Lambda = \{\lambda_i : \lambda_i \in C, i = 1, 2, \ldots, n\}$. The parametric eigenvalue assignment relies on rewriting

$$(\lambda_i I - A)\boldsymbol{v}_i = B\boldsymbol{u}_i \tag{20}$$

in matrix format as

$$\bar{A}V = \bar{B}U \tag{21}$$

or

$$[\bar{A} \quad -\bar{B}] \begin{bmatrix} V \\ U \end{bmatrix} = 0 \tag{22}$$

where

$$\bar{A} = \begin{bmatrix} (\lambda_1 I - A) & & & \\ & (\lambda_2 I - A) & & \\ & & \ddots & \\ & & & (\lambda_n I - A) \end{bmatrix} \tag{23}$$

$$\bar{B} = \begin{bmatrix} B & & & \\ & B & & \\ & & \ddots & \\ & & & B \end{bmatrix} \tag{24}$$

The crucial step is to do the singular value decomposition

$$[\bar{A} \quad -\bar{B}] = X\Sigma Y^H \tag{25}$$

where

$$\Sigma = \begin{bmatrix} \Sigma_{11} & 0 \\ 0 & 0 \end{bmatrix} \tag{26}$$

where $\Sigma_{11} \in R^{\rho \times \rho}$ is nonsingular, ρ is the rank of Σ, X and Y are unitary matrices partitioned conformably with Σ, and Y^H is the complex conjugate transpose of Y. It follows that

$$\begin{bmatrix} V \\ U \end{bmatrix} = Y \begin{bmatrix} 0 \\ \Delta \end{bmatrix}$$

where $\Delta \in R^{(n+m-\rho)\times n}$ is an arbitrary matrix that parameterizes freedom beyond eigenvalue assignment.

Let $V(\Delta)$, $U(\Delta)$ be the solution. Hence,

$$K(\Delta) = -U(\Delta)V^{-1}(\Delta) \tag{27}$$

It can be verified by tedious manipulation that if Λ is a self-conjugate set then K is real. In the computer implementation, we have followed more closely the original development by Liu and Patton,[7] where the arithmetic is kept real.

B. H^∞ Formulation

Clearly, the parameters in the matrix Δ can be chosen arbitrarily. Hence, we choose the parameter matrix Δ to achieve decoupling between the short periodic mode and the phugoid mode. The objective function to be minimized to achieve decoupling is the maximum singular value of a frequency-weighted transfer matrix incorporating transmissions from actuators to tracking errors, transmissions from actuators to outputs to be decoupled from actuators, as well as transmissions from some initial conditions to outputs to be decoupled from initial conditions. When these guidelines are followed, the generic performance optimization problem can be described as follows:

$$\min_{\Delta=\{\delta_{ij}\}} \|W(s)\{CT[sI - A + BK(\Delta)]^{-1}B_{\text{in}} + D\}\|_\infty \tag{28}$$

In Eq. (28), $\Delta = \{\delta_{ij}\}$ is the matrix of free parameters, for $i = 1, 2, \ldots, n+m-\rho$ and $j = 1, 2, \ldots, n$. T is a diagonal scaling matrix to adjust the desired scalings from the unit step actuator inputs to the steady-state responses. C is a matrix specifying the controlled variables. D is a matrix that sets up the tracking/disturbance rejection requirements. It is made up of 0s and -1s. A row of 0s introduces a disturbance rejection term whereas a -1 introduces a tracking error term between the actuator corresponding to the column position of -1 and the output corresponding to the row position of -1. $W(s)$ is the frequency-dependent weighting matrix. B_{in} is a modified B matrix to allow some initial conditions to be treated as disturbances.

Here we focus on the design objective of obtaining a good tracking performance between the angle of attack and the symmetric elevon and a good rejection of an angle-of-attack initial condition. The B, B_{in}, CT, D, and $W(s)$ matrices are chosen as follows:

$$B = \begin{bmatrix} \boldsymbol{b}_{r_e} & \boldsymbol{b}_{r_\eta} \end{bmatrix}, \qquad B_{\text{in}} = \begin{bmatrix} \boldsymbol{b}_{r_\eta} & \boldsymbol{b}_i \end{bmatrix}$$

$$\boldsymbol{b}_i = [0 \quad 0.05 \quad 0 \quad 0 \quad 0 \quad 0 \quad 0]^T$$

$$CT = [0 \quad 100 \quad 0 \quad 0 \quad 0 \quad 0 \quad 0], \qquad D = [0 \quad 0]$$

$$W(s) = \frac{\omega_2 s}{s^2 + (\omega_1 + \omega_2)s + \omega_1\omega_2}$$

$$\omega_1 = 0.01 \text{ rad/s}, \qquad \omega_2 = 1 \text{ rad/s}$$

It turns out that good performance is achieved by this simple, but carefully chosen, performance function. In the preceding matrices, $\boldsymbol{b}_i$ is introduced to emulate an angle-of-attack initial condition input. The controlled output, specified by CT, is obviously the angle of attack. Most important, $W(s)$ is a weighting from 0.01 to 1 rad/s covering the phugoid mode. It is designed to reject the slow phugoid component in the angle-of-attack response, so that the dynamics of the angle-of-attack response would follow the (fast) short periodic. This is a specific manifestation of the short periodic/phugoid decoupling requirement.

C. Genetic Algorithm Solution

To solve the preceding optimization problem, we use genetic algorithms as described in Refs. 10 and 11. The genetic algorithm for this problem is typically implemented as follows (e.g., see Ref. 12).

1) Find the parametric expressions of the closed-loop eigenvector matrix V and the full state feedback K. These expressions are in terms of the matrix Δ. Then the problem to be addressed is to

define an objective function that indicates the fitness of any potential solution. The fitness function is

$$J(\Delta) = -\|W(s)\{CT[sI - A + BK(\Delta)]^{-1}B_{\text{in}} + D\}\|_\infty \quad (29)$$

2) A population of candidate solutions subject to the eigenvalue constraints is initialized. Typically, each trial solution is coded as a chromosome $c_k = \{\delta_{ij,k}\}$, where $\{\delta_{ij,k}: i = 1, 2, \ldots, n + m - \rho$ and $j = 1, 2, \ldots, n\}$ is the set of parameters left beyond eigenvalue assignment of the kth trial solution. The objective is to find the maximum fitness chromosome c^* defined as

$$J[\Delta(c^*)] = \max_k J[\Delta(c_k)] = \max_k \Big[-\|W(s)\Big(CT\{sI - A + BK[\Delta(c_k)]\}^{-1}B_{\text{in}} + D\Big)\|_\infty\Big] \quad (30)$$

Then keep a copy of the maximum fitness chromosome c^* to be reinstalled in the chromosome set of the next generation.

3) Each chromosome c_i is assigned a probability of reproduction, $p(c_i)$, $i = 1, \ldots, M$, proportional to its fitness relative to the other chromosomes in the population. Let the parameter r be the ranking of the individual chromosomes, where $r = 1$ is the maximum fitness

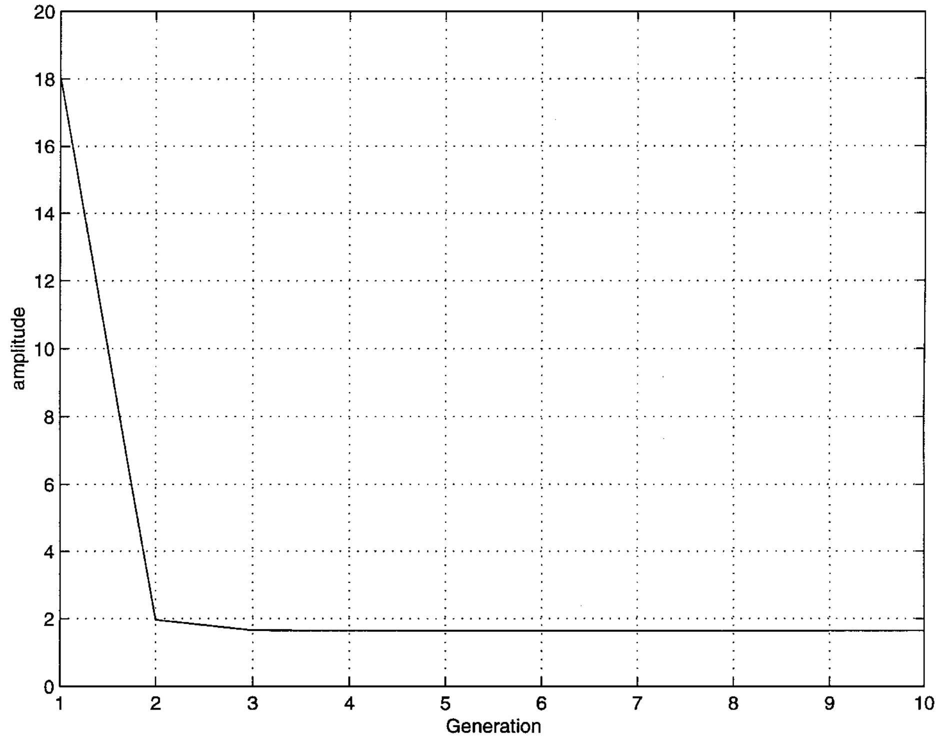

Fig. 2 Evolution of the maximum of the H^∞ norms of all error transfer matrices as a function of the generation.

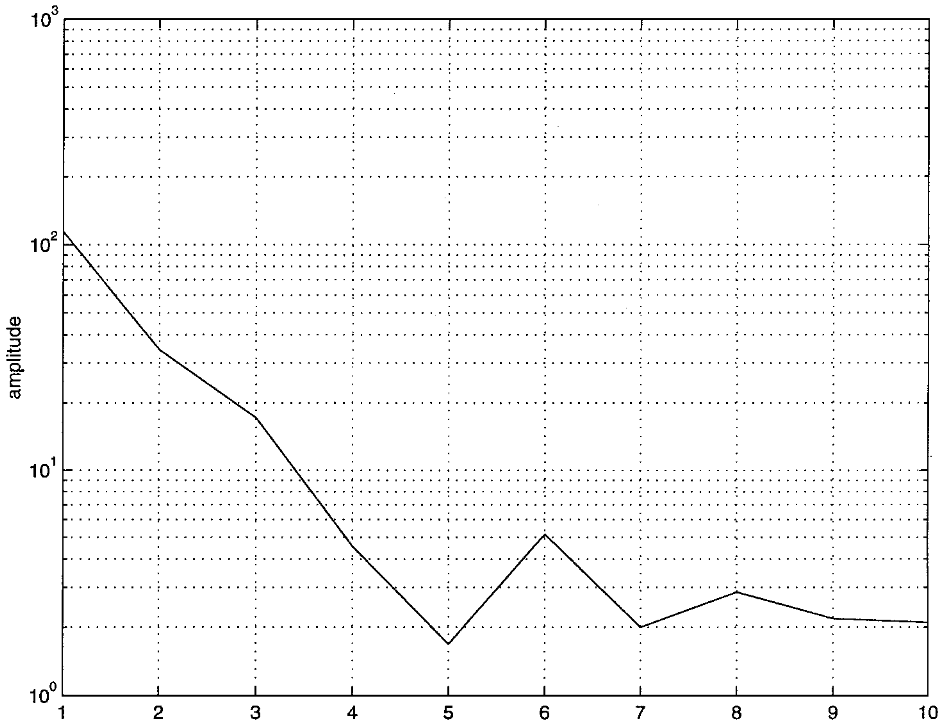

Fig. 3 Evolution of the average of the infinity norms of all error transfer matrices as a function of the generation.

chromosome. Let the parameter q be the geometric selection constant. Then the probability of reproduction for the rth chromosome c_r is

$$p(c_r) = \{q/[1-(1-q)^M]\} \cdot (1-q)^{r-1} \tag{31}$$

The parameter q has the simple interpretation as the probability of reproduction of the best individual since

$$p(c_1) = q/[1-(1-q)^M] \approx q \tag{32}$$

when the population size M is sufficiently large. This selection method is called normalized geometric selection.

4) According to the assigned probabilities of reproduction, $p(c_i)$, $i = 1, \ldots, M$, a new population of chromosomes is generated by probabilistically selecting strings from the current population. The selected chromosomes generate offsprings via the use of specific genetic operators, such as crossover and mutation operators. Crossover operators are applied to two chromosomes (parents) and creates two new chromosomes (offsprings). There are three crossover operators used in this problem.

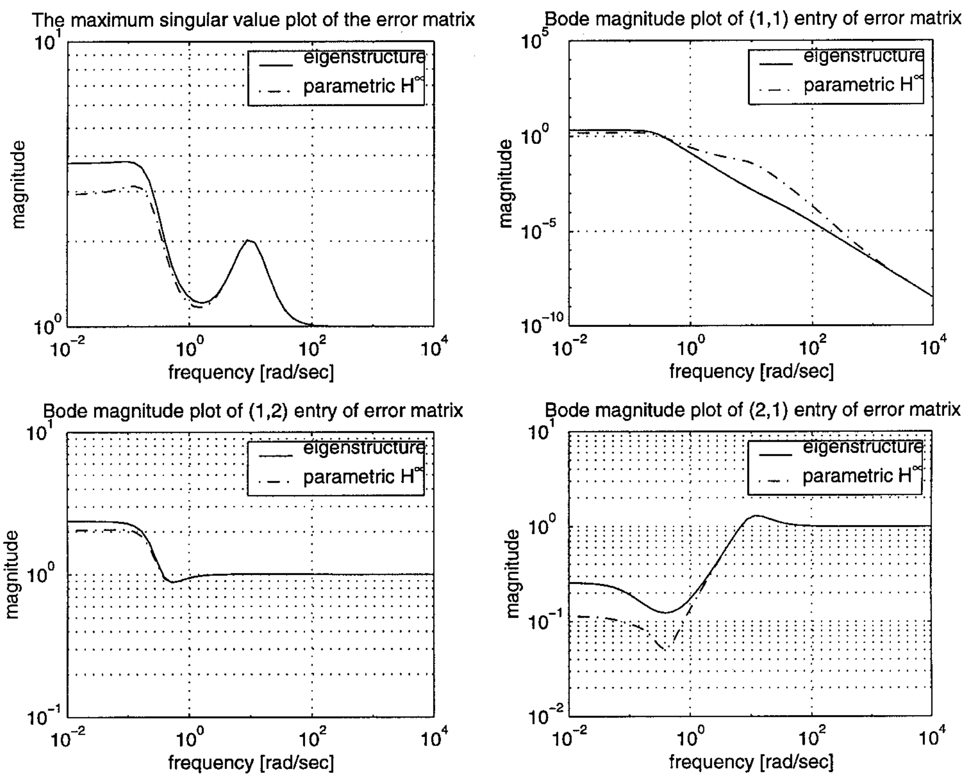

Fig. 4 First set of frequency responses of error transfer matrix.

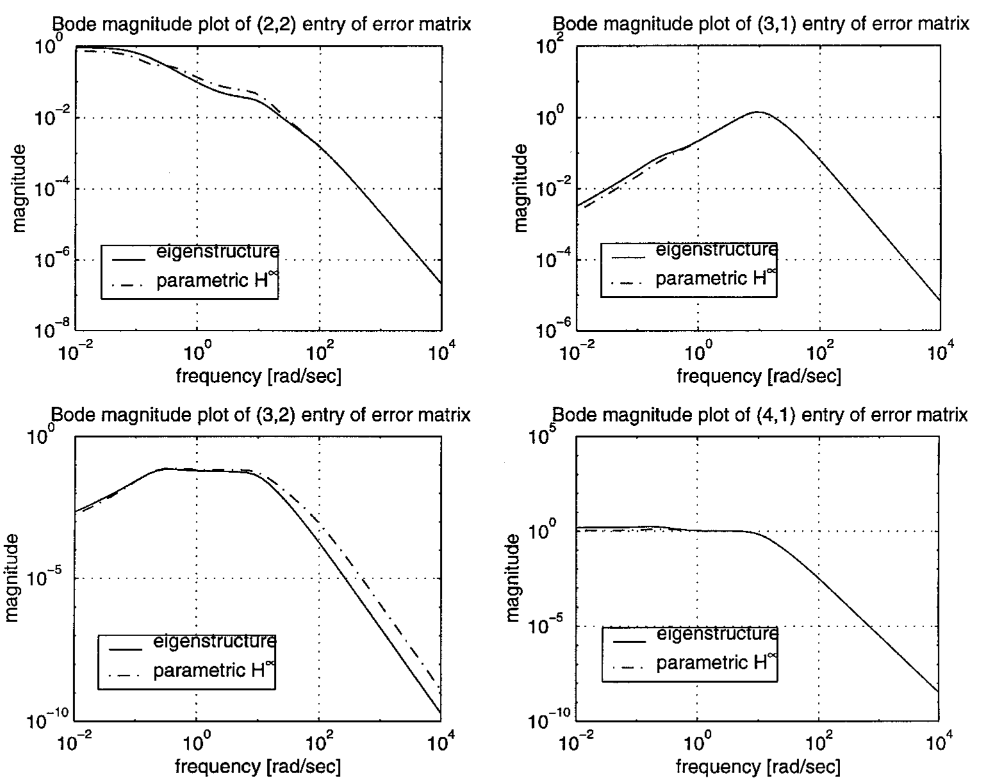

Fig. 5 Second set of frequency responses of error transfer matrix.

The first crossover operator is simple crossover. This operator is defined as follows: If $c_1 = (v_1, \ldots, v_L)$ and $c_2 = (w_1, \ldots, w_L)$ are the chromosomes selected to crossover, then the resulting offsprings are $\tilde{c}_1 = (v_1, \ldots, v_r, w_{r+1}, \ldots, w_L)$ and $\tilde{c}_2 = (w_1, \ldots, w_r, v_{r+1}, \ldots, v_L)$, where r is uniformly randomly selected between 1 and $L - 1$.

The second crossover operator is the arithmetic crossover. This operator is defined as follows: If $c_1 = (v_1, \ldots, v_L)$ and $c_2 = (w_1, \ldots, w_L)$ are the chromosomes selected to crossover, then the resulting offsprings are $\tilde{c}_1 = a \cdot c_1 + (1 - a) \cdot c_2$ and $\tilde{c}_2 = (1 - a) \cdot c_1 + a \cdot c_2$, where the number a is uniformly randomly selected between 0 and 1.

The third crossover operator is the heuristic crossover. This operator is defined as follows: If $c_1 = (v_1, \ldots, v_L)$ and $c_2 = (w_1, \ldots, w_L)$ are the chromosomes selected to crossover, with the fitness of c_1 greater than the fitness of c_2, then the resulting offsprings are

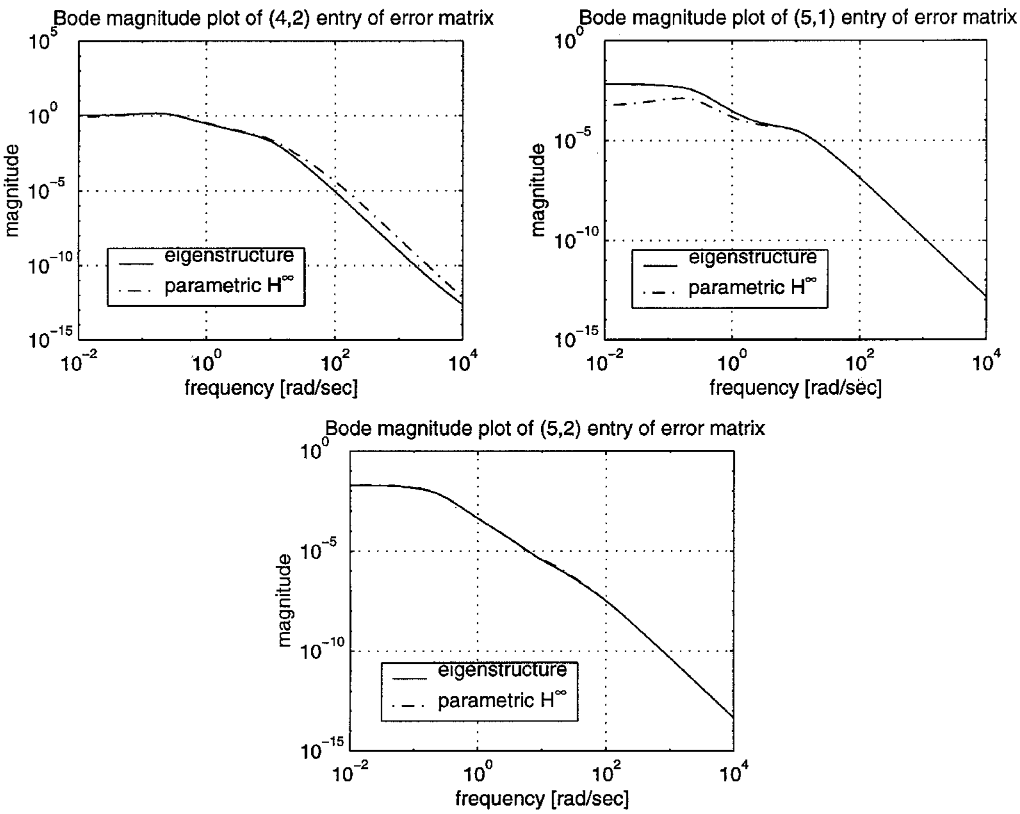

Fig. 6 Frequency responses of error transfer matrix.

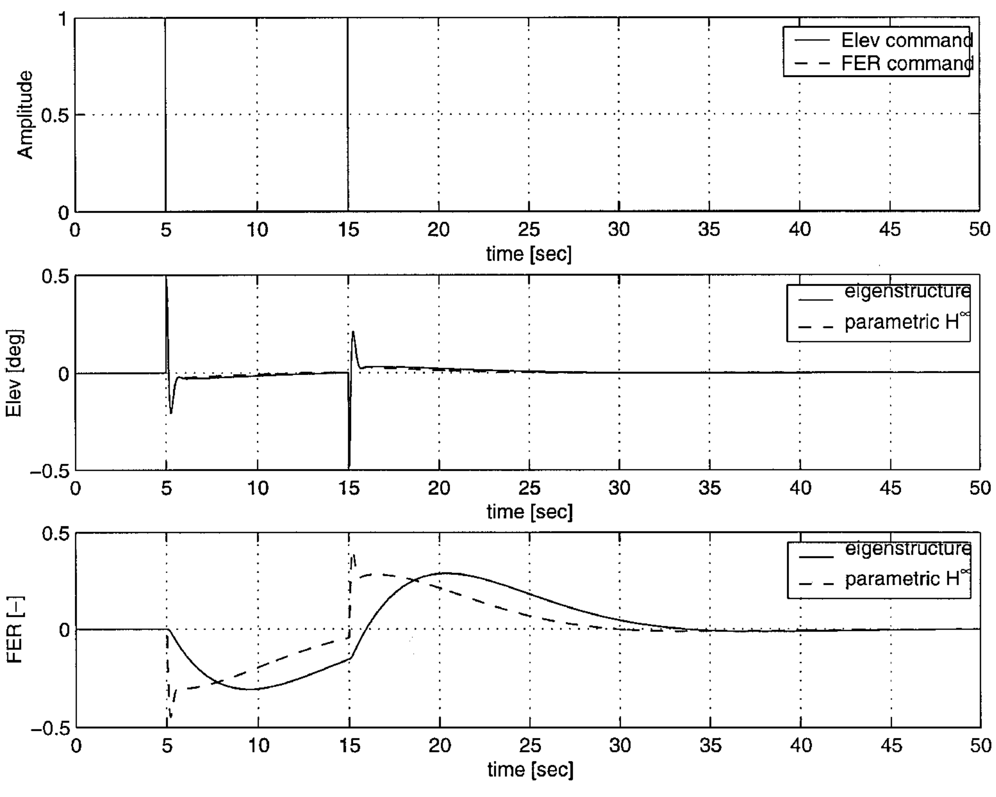

Fig. 7 Elevon and FER time-domain responses to elevon command.

$\tilde{c}_1 = c_1 + a \cdot (c_1 - c_2)$ and $\tilde{c}_2 = c_1$, where the number a is a uniformly distributed random number between 0 and 1.

On the other hand, mutation operators are applied to one chromosome (parent) and create a new chromosome (offspring). There are two mutation operators used in this problem.

The first mutation operator is uniform mutation. This operator is defined as follows: If $c_1 = (v_1, \ldots, v_L)$ is the chromosome selected for mutation, then the resulting chromosome is $\tilde{c}_1 = (v_1, \ldots, v_{r-1}, \acute{v}_r, v_{r+1}, \ldots, v_L)$, where $\acute{v}_r$ is a random variable uniformly distributed over from the interval $[L_r, U_r]$ of the corresponding rth parameter where U_r and L_r are the upper bound and the lower bound, respectively, of the domain of the parameter v_r. The number r is a random number uniformly distributed between 1 and L.

The second mutation operator is boundary mutation. This operator is defined as follows: If $c_1 = (v_1, \ldots, v_L)$ is the chromosome

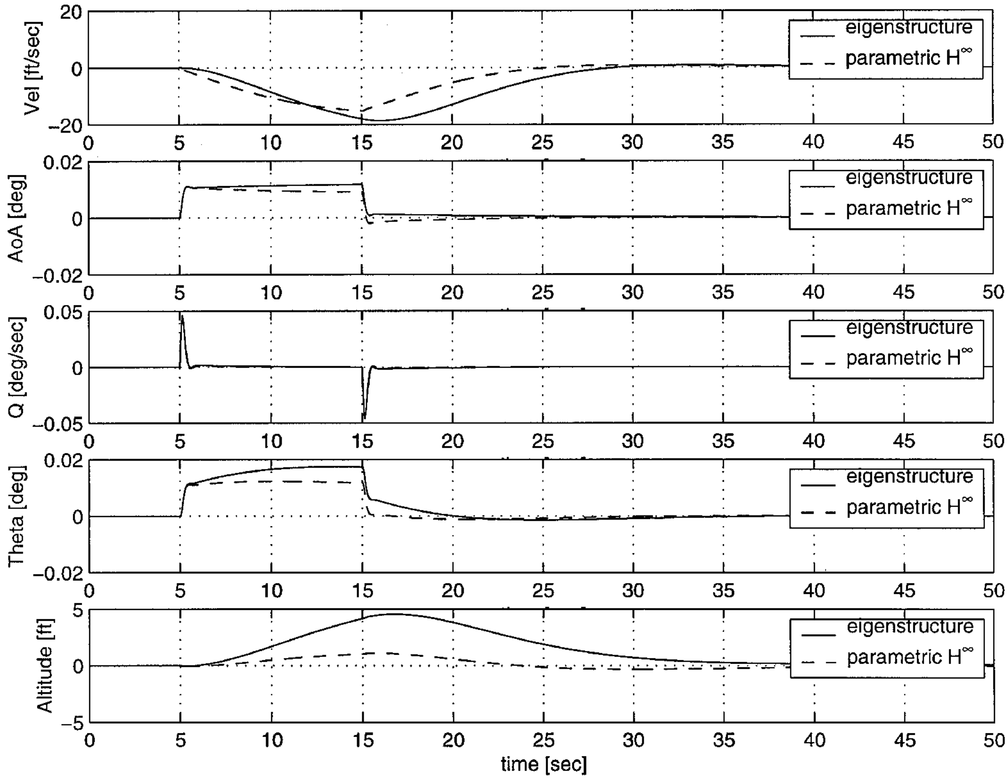

Fig. 8 Velocity, angle-of-attack, pitch-rate, pitch-angle, and altitude time-domain responses to elevon command.

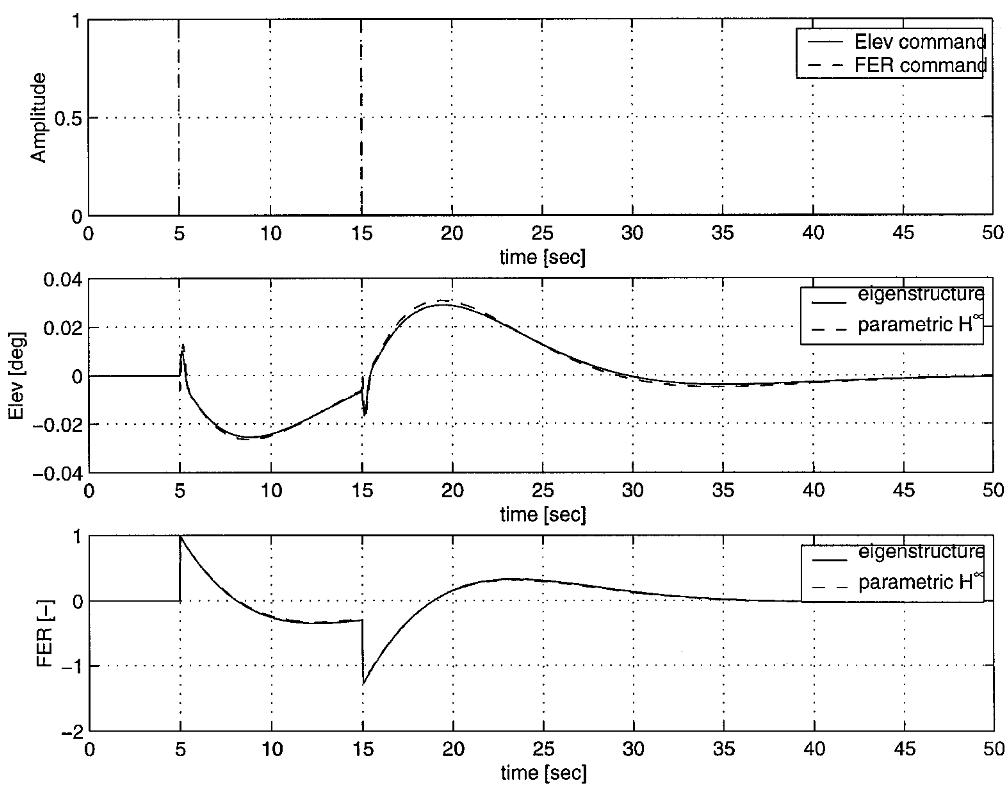

Fig. 9 Elevon and FER time-domain responses to FER command.

selected for mutation, then the resulting chromosome is $\tilde{c}_1 = (v_1, \ldots, v_{r-1}, \acute{v}_r, v_{r+1}, \ldots, v_L)$, where

$$\acute{v}_r = \begin{cases} U_r & \text{if} \quad a \geq 0.5 \\ L_r & \text{if} \quad a < 0.5 \end{cases}$$

The number a is a uniform random number between 0 and 1. The number r is a uniform random number between 1 and L. The parameters U_r and L_r are the upper bound and the lower bound, respectively, of the domain of the parameter v_r.

5) Replace the worst chromosome in the new population by the best chromosome c^* in the previous generation.

6) The process is stopped if a suitable solution of acceptable fitness has been found or if the available computing time has expired; otherwise, the process proceeds to step 2, where the new chromosomes are scored and the cycle is repeated.

7) Synthesize the controller K by using the optimal chromosome.

The parameters of this genetic algorithm are shown in Table 3. The resulting evolution of the infinity norm of the error transfer matrix over the generations is shown in Figs. 2 and 3.

The problem with genetic algorithms is how to choose the parameters of the genetic algorithm. Because the theoretical convergence results rely on the hypothesis of infinite population size and infinitely many generations, the selection criteria for the parameters of the crossover and the mutation operations to guarantee a global optimum are not known. Moreover, the parameters of the crossover and the mutation operations affect the rate of the convergence and could lead to premature convergence of the genetic algorithm. In this particular simulation, a specific problem is that, although the genetic algorithm converges after a very few generations, it is computationally very intensive for each generation. This problem is due to the complexity of the fitness function. In this problem, the fitness function is the infinity norm of the error transfer matrix. The computation of the fitness function involves the computation of the supremum over all frequencies of the maximum singular value of this transfer matrix using a bisection method. This creates a serious computational burden in the Matlab® implementation, resulting in a slow genetic algorithm.

We note that another computational implementation of the Shapiro eigenstructure assignment is provided by the geometric decoupling problem.[13,14]

Table 3 Parameters of the genetic algorithm

Parameter	Value
Number of generation	10
Population size	100
Geometric selection constant	0.3
Number of retries for heuristic crossover	3
Arithmetic crossover	20 per generation
Heuristic crossover	20 per generation
Simple crossover	20 per generation
Uniform mutation	5 per generation
Boundary mutation	5 per generation

V. Simulation Results and Interpretation

The full state feedback gain matrices K, for both the eigenstructure and the constrained H^∞ approaches, are shown in Table 4. The various frequency response plots of the error transfer matrix,

$$CT(sI - A + BK)^{-1}B + D = \begin{bmatrix} \dfrac{0.1v}{r_e} & \dfrac{0.1v}{r_\eta} - 1 \\ \dfrac{100\alpha}{r_e} - 1 & \dfrac{100\alpha}{r_\eta} \\ \dfrac{20q}{r_e} & \dfrac{20q}{r_\eta} \\ \dfrac{100\theta}{r_e} & \dfrac{100\theta}{r_\eta} \\ \dfrac{0.001h}{r_e} & \dfrac{0.001h}{r_\eta} \end{bmatrix}$$

Table 4 Controller gain matrices

Method	Controller gain matrix K					
Eigenstructure	−0.0065	105.2929	13.0113	−8.7237	−0.0499	0.4935	−0.0027
	0.0371	−93.5424	2.8952	94.6092	0.0682	−0.0004	0.0147
Parametric H^∞	−0.0114	102.0694	13.3835	−5.2256	−0.0391	0.4985	0.0199
	0.0341	−53.4998	8.6776	85.1538	0.0476	0.1114	0.0132

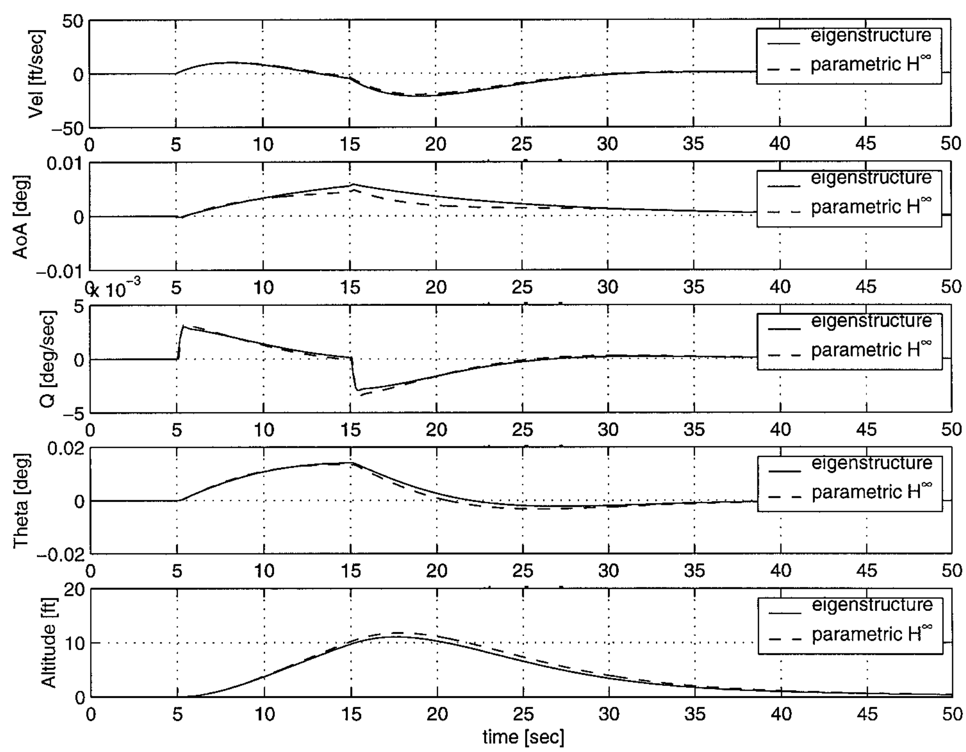

Fig. 10 Velocity, angle-of-attack, pitch-rate, pitch-angle, and altitude time-domain responses to FER command.

for both the eigenstructure and the constrained H^∞ method, are shown in Figs. 4–6. The time-domain responses for both methods are shown in Figs. 7–12.

First, observe the surprising consistency between the respective entries of the gain matrices of the eigenstructure and the constrained H^∞ approaches.

Next, it is easily seen that, except for a very few minor exceptions, constrained H^∞ optimization does a better job at shaping the frequency response of the error transfer matrix. This is not surprising, because H^∞ directly shapes the frequency response whereas eigenstructure does it quite indirectly. More specifically, observe that the maximum singular value of the error transfer matrix for the parametric H^∞ design is lower at low frequency than for the eigenstructure design. This is because the parametric H^∞ design error function is weighted with a low-pass filter $W(s)$.

Regarding the time-domain responses, the two methods are nearly perfectly aligned (despite their quite different design methodologies) as fas as control of the velocity by FER and response to

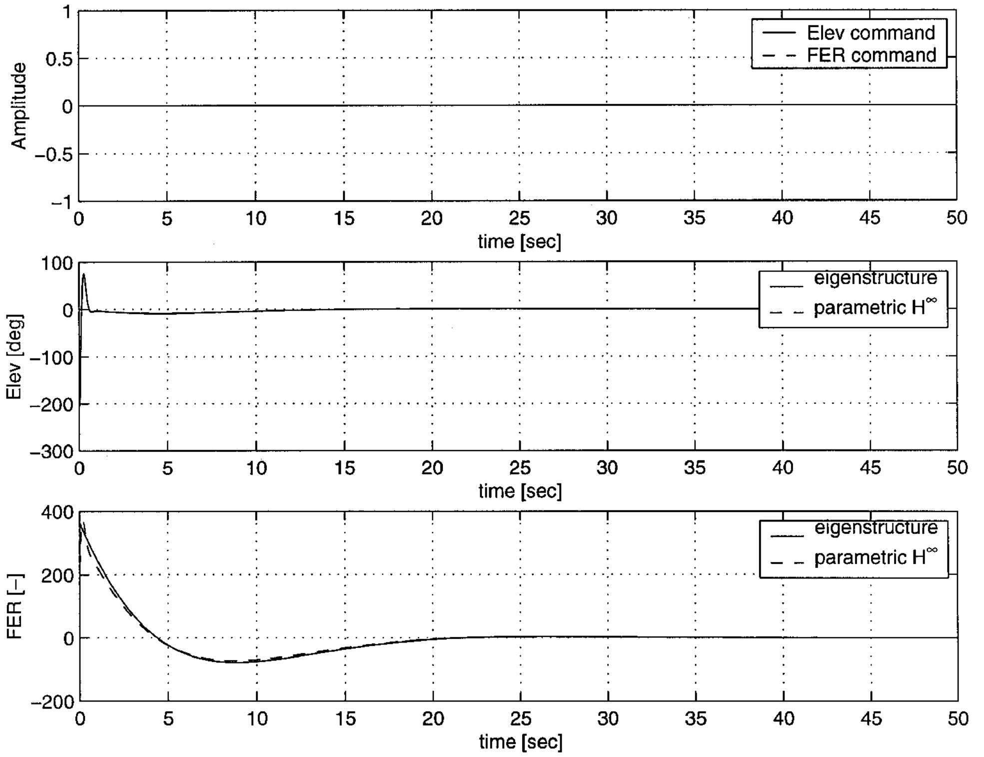

Fig. 11 Elevon and FER time-domain responses to angle-of-attack initial condition.

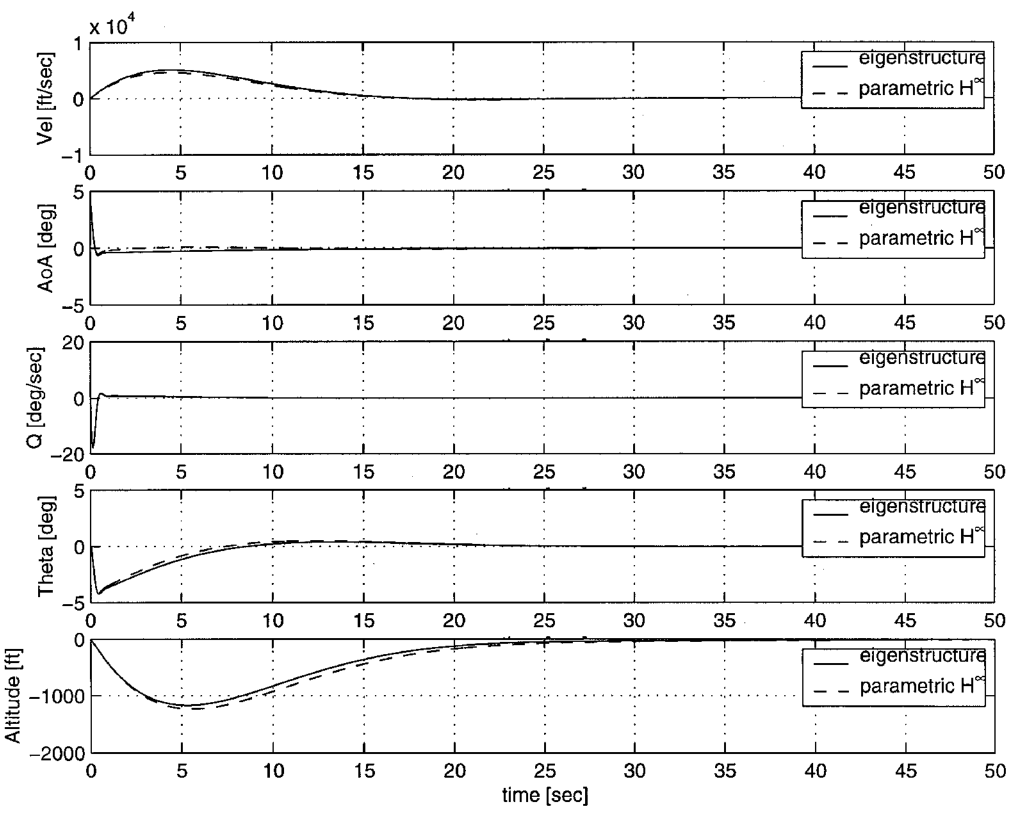

Fig. 12 Velocity, angle-of-attack, pitch-rate, pitch-angle, and altitude time-domain responses to angle-of-attack initial condition.

angle-of-attack initial condition are concerned. However, the new method works markedly better at controlling the angle of attack by elevon. Also, better control of the pitch angle (and, hence, of the altitude via the relation $\gamma = \theta - \alpha$) is achieved.

Clearly, this case study is an angle-of-attack tracking maneuver at constant altitude, which in turn requires the pitch angle to follow the angle of attack along with a velocity drop. The altitude holding is basically due to the altitude eigenvalue being assigned the stable value of -0.1 (see Table 1). Relaxing this latter constraint to allow for a marginally stable altitude eigenvalue and using the same overall philosophy produces a climb maneuver.

VI. Conclusions

Whereas the Shapiro eigenstructure assignment relies on elementary linear algebra and has been successfully used in such designs as the lateral control of the B-2, it nevertheless incorporates many subtle points that the present paper has attempted to pin down. Duplicating, a fortiori out performing, eigenstructure assignment by H^∞ methods can only be done at the expense of a careful choice of the transfer matrix to be minimized, combined with a careful choice of the frequency weighting. From a deeper theoretical point of view, eigenstructure assignment is in fact a geometric decoupling problem, to which the Shapiro algorithm only provides intuitive approximate solution.

Acknowledgments

This research was supported by the National Science Foundation, Grant 98-02594, and NASA Marshall Space Flight Center, Grant NAS8-97292.

References

[1]Mankins, J. C., “Lower Costs for Highly Reusable Space Vehicles,” *Aerospace America*, Vol. 36, No. 3, 1998, pp. 36–42.

[2]Wilson, J. R., “X-33 and RLV Take Parallel Paths,” *Aerospace America*, Vol. 37, No. 2, 1999, pp. 38–42.

[3]Buschek, H., “Synthesis of Fixed Order Controllers with Robustness to Mixed Real/Complex Uncertainties,” Ph.D. Thesis, Dept. of Aerospace Engineering, Georgia Inst. of Technology, Atlanta, GA, Feb. 1995.

[4]Raney, D. L., Phillips, M. R., and Person, L. H., Jr., “Investigation of Piloting Aids for Manual Control of Hypersonic Maneuvers,” NASA TP 3525, 1995.

[5]Vu, P., and Biezad, D. J., “Direct-Lift Design Strategy for Longitudinal Control of Hypersonic Aircraft,” *Journal of Guidance, Control, and Dynamics*, Vol. 17, No. 6, 1994, pp. 1260–1266.

[6]McIver, D. E., and Morrel, F. R., “National Aero-Space Plane-Flight Mechanics,” CP-489, AGARD, June 1990.

[7]Liu, G. P., and Patton, R. J., “Parametric State Feedback Controller Design of Multivariable Systems,” *International Journal of Control*, Vol. 61, No. 6, 1995, pp. 1457–1464.

[8]Liu, G. P., and Patton, R. J., “Robust Control Design Using Eigenstructure Assignment and Multi-Objective Optimization,” *International Journal of Systems Science*, Vol. 27, No. 9, 1996, pp. 871–879.

[9]Liu, G. P., and Patton, R. J., “Robust Control Design Based on Parametric Eigenvalue Assignment,” *International Journal of Systems Science*, Vol. 29, No. 1, 1998, pp. 65–74.

[10]Goldberg, D. E., *Genetic Algorithms in Search, Optimization, and Machine Learning*, Addison Wesley Longman, Reading, MA, 1989, pp. 27–86.

[11]Michalewicz, Z., *Genetic Algorithms + Data Structure = Evolution Programs*, 3rd ed., Springer-Verlag, New York, 1996, pp. 13–55, 97–108.

[12]Houck, C. R., Joines, J. A., and Kay, M. G., “A Genetic Algorithm for Function Optimization: A Matlab Implementation,” Dept. of Industrial Engineering, North Carolina State Univ., TR NCSU-IE 95-09, Raleigh, NC, 1995.

[13]Moore, B. C., and Silverman, L. M., “Model Matching by State Feedback and Dynamic Compensation,” *IEEE Transactions on Automatic Control*, Vol. 17, No. 4, 1972, pp. 491–497.

[14]Jonckheere, E. A., and Lohsoonthorn, P., “A Geometric Approach to Model Matching Reconfigurable Propulsion Control,” *Proceedings of the American Control Conference*, IEEE Publications, Piscataway, NJ, 2000, pp. 2388–2392.